尚唯信息
SUNWAYINFO

尚唯科技报告资源服务系统

重庆尚唯信息技术有限公司

CHONGQING SUNWAY INFORMATION TECHNOLOGY CO.,LTD

【一】/ 公司介绍

重庆尚唯信息技术有限公司隶属于原科技部西南信息中心，成立于 2002 年 6 月，是一家专业从事科研大数据研发和文本智能处理为核心的高新技术企业，致力于中英文大数据产品的开发、设计、营销与服务。公司拥有成熟的数字文献资源一体化解决方案，是我国专业的数字资源信息供应商。

公司拥有独具特色的系列特种文献数据库产品，包括：《尚唯产品样本数据库》、《尚唯科技报告资源服务系统》、《尚唯军用标准信息服务平台》、《全球智库发现系统》、《尚唯职业教育在线学习系统》、《工程技术数据库》、《航空航天及汽车工业技术资料系统》、《尚唯学位论文文献服务系统》、《国外标准集成发现系统》、《智能制造服务平台》等，并通过统一检索系统“尚唯特种知识服务平台”实现统一检索和服务。此外，随着客户需求的日益变化，公司积极布局转型业务网络，参与众多合作项目，形成覆盖数据采集与清洗、专题文献库建设、特色平台开发等多方面的业务体系，以强大的技术实力满足客户多样化需求。

目前，公司已拥有中国科学院文献情报中心、清华大学、浙江大学、中国科技大学、中山大学、国防科技大学、解放军信息工程大学、天津市科技情报研究所等数百家涵盖高等院校、情报研究所、科研机构、企事业单位和公共图书馆领域的用户，已经形成以产品与系统建设为核心的一大批忠实用户群，逐步建立起自己的品牌效应与业务优势。

经过多年发展，公司拥有 22 项知识产权证书，通过了“知识产权管理体系认证”和“ISO 质量管理体系认证”，是 3A 级信用企业，重庆市软件企业，2018 年参与了总投资规模达到 4000 万元的国家重点研发计划“专业内容知识服务众智平台与应用示范”项目的建设。

公司资质：

【二】/ 产品概述

访问地址：http://bg.sunwayinfo.com.cn/

《尚唯科技报告资源服务系统》主要收录国外科技报告，为用户提供科技报告这一特种文献的一站式检索查询、原文传递以及信息挖掘服务。

科技报告是描述科研活动的过程、进展和结果，并按照规定格式编写的科技文献，能够完整且真实的反映科研机构或人员所从事科研活动的内容和经验，是国家基础性、战略性科技资源，也是国家科技实力的重要体现。

◆ **报告来源：**美国四大报告（航空航天局的 NASA 报告、能源部的 DE 报告、国防部的 AD 报告、商务部的 PB 报告），以及美国国家科学院、日本宇宙航空研究开发机构、荷兰国家学术研究与合作信息系统、IBM 公司、兰德公司、加州大学伯克利分校、哥伦比亚大学、UNT 数字图书馆、美国国家农业图书馆、世界银行组织、国际货币基金组织等机构。

◆ **收录量：**题录文摘收录量已超过 485 万个记录，能够获取的报告全文数量已超过 370 万篇，每年新增约 3-5 万份报告。

◆ **分类体系：** 提供主题分类，将报告分为 32 个一级分类，向下分为 347 个二级分类，以及 707 个三级分类。

◆ **收录年限：**1900 年至今。

◆ **数据更新：**中心网站和镜像站季度更新。

◆ **全文格式：**PDF 文档。

◆ **标引字段：**报告名称、报告号、作者、主题分类、研究机构、赞助机构、关键词、发布年份、文献类型、合同编号、语言、页数、摘要等。

◆ **检索方式：**快速检索、高级检索、主题分类导航、研究机构导航、科研项目导航等。

【三】/ 核心优势

1

海量数据信息

该库是目前收录国外科技报告数量最多的数据库，集科技报告题录文摘、全文文献信息，以及科研项目信息于一体，其中题录已超过 485 万条，全文 370 万篇，科研项目 252 万余个，资源量大，数据更新快。

2

回溯年代长

该库收录年代久远，回溯了从 1900 年至今的科技报告。通过回溯极大丰富了资源内容，可以访问整个研究进程所有可用的文献，是探索科研活动进程和结果的重要途径，为科研带来更多可能性，让科研过程高效省时。

3

权威文献来源

该库收录了众多知名来源机构的报告，如美国四大报告、欧洲投资基金、国际货币基金组织、世界银行、兰德公司、加州大学伯克利分校等，是掌握科学技术前沿信息的有力资源。

4

题录信息完整

提供报告标题、作者、关键词、摘要、主题分类、报告号、合同编号、文献类型、发布日期、报告涵盖时间、研究机构、赞助机构、合作机构、基金编号、国别、语种等具体字段展示，题录信息完整而丰富。

5

深度关联，信息全面

该库对科研项目信息进行了分类整理，方便查询科研项目研究内容、资金投入等内容，掌握项目的整体研究情况；全方位展示研究机构信息，以及机构之间的关联性，并对机构报告进行分类展示，搜索过程更加便捷，搜索结果更加精准。

【四】/ 新版特色

1、挖掘底层数据展示隐藏信息

通过对科技报告现有数据字段的梳理，对不同来源的数据字段进行合并处理，对不规范字段进行统一化处理，并补齐更多字段信息，如主题分类、合同编号、报告涵盖时间、赞助机构、基金编号等字段，更加详细的展示文献资源信息，帮助用户探索更多隐藏内容。

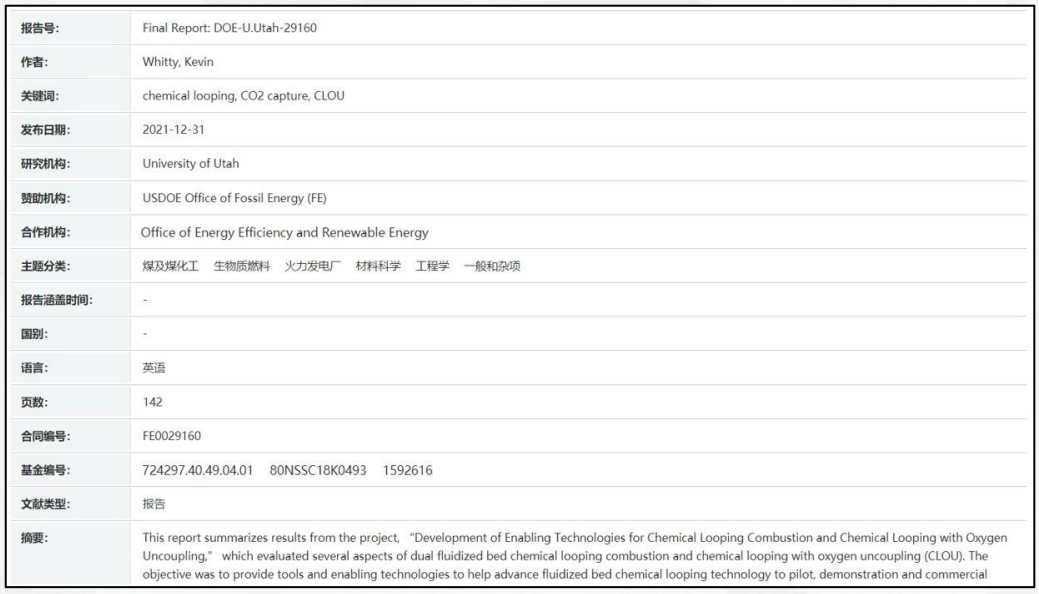

报告号:	Final Report: DOE-U.Utah-29160
作者:	Whitty, Kevin
关键词:	chemical looping, CO2 capture, CLOU
发布日期:	2021-12-31
研究机构:	University of Utah
赞助机构:	USDOE Office of Fossil Energy (FE)
合作机构:	Office of Energy Efficiency and Renewable Energy
主题分类:	煤及煤化工　生物质燃料　火力发电厂　材料科学　工程学　一般和杂项
报告涵盖时间:	-
国别:	-
语言:	英语
页数:	142
合同编号:	FE0029160
基金编号:	724297.40.49.04.01　80NSSC18K0493　1592616
文献类型:	报告
摘要:	This report summarizes results from the project, "Development of Enabling Technologies for Chemical Looping Combustion and Chemical Looping with Oxygen Uncoupling," which evaluated several aspects of dual fluidized bed chemical looping combustion and chemical looping with oxygen uncoupling (CLOU). The objective was to provide tools and enabling technologies to help advance fluidized bed chemical looping technology to pilot, demonstration and commercial

展示字段及其说明如下：

展示字段名	说明
标题	标明报告内容的简短语句
作者	报告撰写人员名称
报告号	标识科技报告的完整的格式化的一组代码
摘要	报告整体的构成与主要内容的简单摘抄
关键词	报告重点内容的概括与总结
发布日期	报告的发布日期
研究机构	参与报告研究、写作的机构
赞助机构	提供资金，用以支持报告、科研的机构
合作机构	合作参与报告研究、写作的机构
主题分类	根据四大报告（DOD、PB、DOE、NASA）的分类特点融合整理出的一套完整的报告分类方式
报告涵盖时间	该篇报告写作的背景时间
国别	报告的归属国籍
语言	报告撰写使用的主要国家语言
页数	报告的全文页数
合同编号	同其他单位签订的合同/合同书的编号
基金编号	支持该报告研究的基金项目编号
文献类型	该字段放通用字段最后，后面紧跟独特字段，逻辑上更有连贯性

2、提取文献类型帮助多维度筛选

由于科研项目周期较长，通常会产生种类繁多的报告类型，通过对其进行技术处理，整理出季度报告、中期报告、最终报告、合同户报告、备忘录、札记、简报等完整的报告类型。此外，还整理了科研项目同时产出的其他文献，有教育出版物、新闻稿、会议文献、期刊论文、学位论文、手册、皮书、标准、专利等多种类型。科技报告与其他文献都是科研项目的共同产物，体现了科研项目成果产出的丰富性。

数据库对每份报告提供类型展示，报告所属类别一目了然，并提供文献类型聚类，进一步方便用户查找所需资源。

报告类型		其他类型	
科技报告	季度报告	其他文献	出版物
	年度报告		会议文献
	中期报告		期刊论文
	最终报告		学位论文
	合同户报告		手册
	备忘录		数据集
	计划文件		标准
	札记		专利
	简报		皮书
	演示稿		新闻稿
	总结报告		图书
	管理报告		多媒体
	技术译文		其他

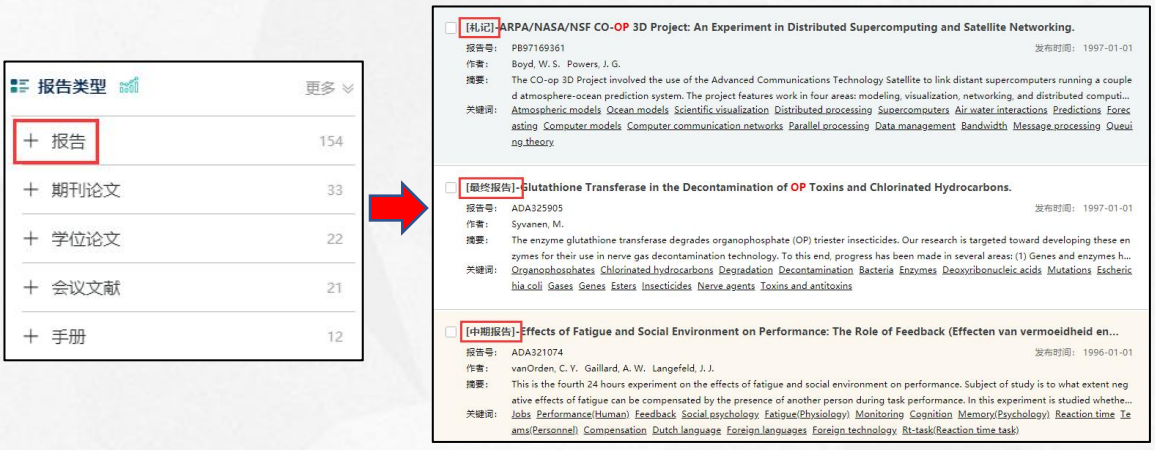

3、知识图谱助力知识发现

提供完整的可视化知识图谱展示，以关系网络节点为基础，在图谱节点之间进行相应探寻，可以发现机构与机构之间的合作关系。此外，也可以发现作者与作者共同发文的共现关系，甄别合作者的研究方向与内容信息。用户还可以对主题分类进行检索，发现不同主题之间的共现网络，为制定科研合作提供参考，从而实现多种应用场景。

举例：以科技报告为检索字段，键入“oil”进行检索，得到以下图谱，以“Four County Permian Basin San Andres Residual Oil Zone(ROZ) Database”为例，通过节点之间的连线组成的可视化图形，可以发现机构合作共现网络，从中分析合作关系与合作次数，从而判断机构合作网络整体联系与紧密程度，能对机构外部合作关系进行科学的度量；此外，也可以发现作者合作网络，顺着合作研究者的研究轨迹对该领域进行更加深入的了解，借此了解特定领域，发现学科生长点，以及寻找自己的合作伙伴，为制定科研合作战略提供参考。

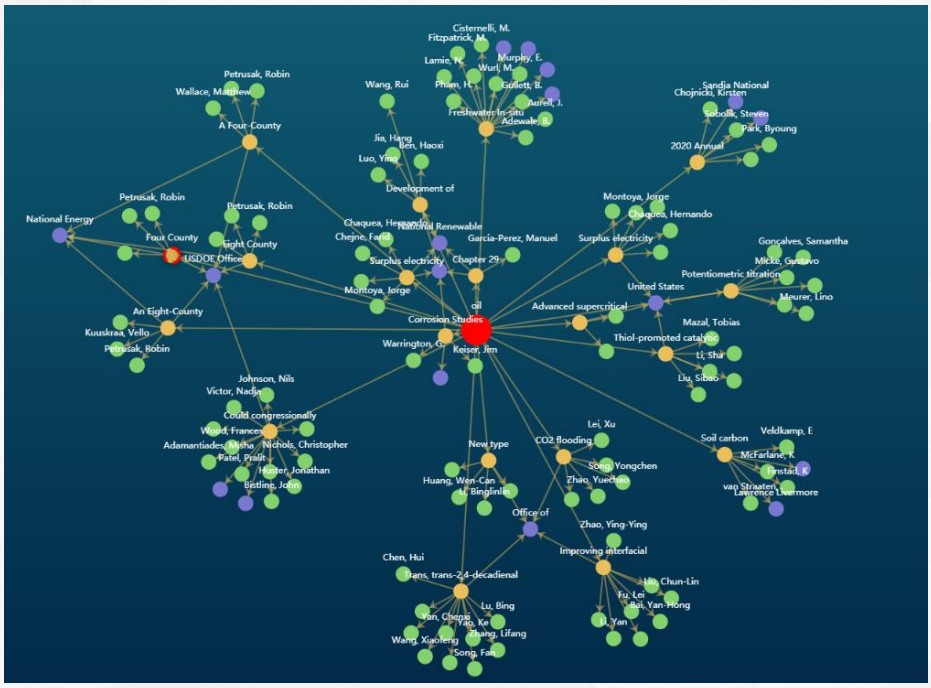

4、构建全新主题分类体系

深度分析科技报告特征，构建贴合科技报告的主题分类体系，涵盖 32 个一级主题，向下分为 347 个二级分类，以及 707 个三级分类，基本囊括主要学科领域，一定程度上揭示了各主题之间的相互联系与相互交叉、相互渗透的关系，便于用户根据主题知识系统，按类检索、查找文献。全部一级主题如下：

材料科学	各国技术译文	化学	工程学
粒子加速器	仪器设备	通讯	电子和电工技术
环境科学	地球科学	航空与空气动力学	探测
物理学	制造技术	天文学和天体物理学	航天
交通运输	建筑技术	图书馆和信息科学	发明许可
农业和食品	商业与经济	计算机、控制与信息理论	一般和杂项
社会科学	军事	城市发展与规划	生物及医学
燃料	新能源	能源与动力工程	数学科学

5、展现科研项目成果全貌

一个完整的科研项目，根据规模和复杂程度，可形成几篇到几十篇、甚至几百上千篇科技报告。

提取科技报告的合同编号进行关联化处理，实现同一项目全部研究成果的关联聚合，揭示科研项目的技术研究过程、方法描述、研制试验结果分析、技术性文件、阶段总结和记录、结果或进展总结等科研成果记录，对掌握项目整体研究全貌有积极作用。

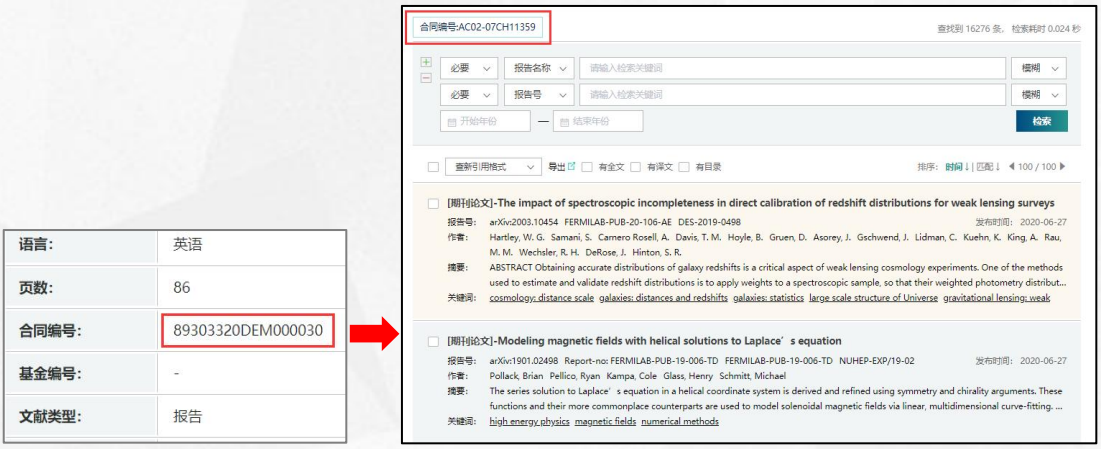

6、全方位展示科研机构信息

通过消歧归一化处理，整理出 3000 余家研究机构，根据机构性质将其划分为企业、实验室、教育机构、研究中心、政府部门等类型，针对不同类型展示相应信息；提供细致到国别、坐标、网址、类型、成立时间等基本信息，以及机构关系、人事信息等相关内容的详细展示，全方位展示研究机构信息。

机构类型		
企业	实验室	政府部门
教育机构	研究中心	其他

数据库提供各类统计图谱，展示机构发文量统计和报告主题分类统计，并对机构报告进行分类展示，各类数据一目了然，并提供各类数据的聚类检索，实现对机构的研究方向和擅长领域的全面深入挖掘。

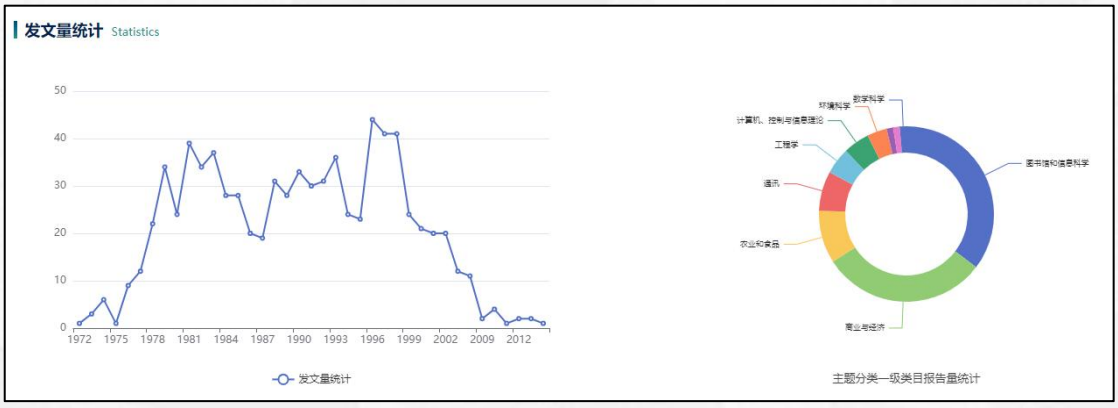

【五】/ 应用价值

◎ 科研立项，科技查新，科学研究

系统收录了国外完整的科技报告资源，以及科研项目信息，能够提供最新资源的查询，具有极高的时效性、客观性、权威性，帮助科研人员实现科技查新，进行科研选题立项，提高科研的起点；在研究遇到问题或瓶颈时，参考科技报告，能够找到解决问题的方向和方法，完成项目研究。

◎ 承接项目，促进创新，积累资产

科技报告是国家权威机构以资助科研项目而形成的产物，能完整积累国际前沿与尖端科学技术的研究成果。系统是目前收录国外科技报告最多的数据库，充分利用其中的文献资源，能帮助高校、研究院与实验室承接国家科技项目，助力技术升级与科技创新；同时，对科技报告的完整保存和充分开发利用，可以避免重复研究，积累技术资产，提高科研效率，提升投入产出效益。

◎ 热点追踪，引用借鉴，参考利用

科技报告涉及到商业经济、航空航天、物理化学、国防军事、工程制造、仪器设备、生物医学等基础科学，以及神经网络、核聚变、量子计算、碳中和、光刻机、电子对抗、暗物质、智能机器人、石墨烯等热点领域和高精尖技术，代表国家科技发展的战略思路和方向；同时，科技报告形成很早，可回溯性强，对研究科技相关领域的发展历程、发展近况以及未来的研究动向都是重要的参考资料。

◎ 结题验收，信息公开，知识共享

在项目中期检查、结题验收阶段形成的科技报告可用于对项目实施进展、过程、成果和真实性进行实时检验，对科技报告的公开或涉限交流，有利于增加科研工作的透明度，杜绝虚假行为，也为社会公众和科技界提供了对科技计划项目成果了解、利用的渠道，提高全社会科技资源的利用效率。

【六】/ 界面功能

1、首页

登录数据库后，首页可进行快速检索操作，并实现对主题分类、研究机构、科研项目、知识图谱和高级检索版块的切换，还包括主题分类、编译报告、科技热词和研究机构等信息展示区。

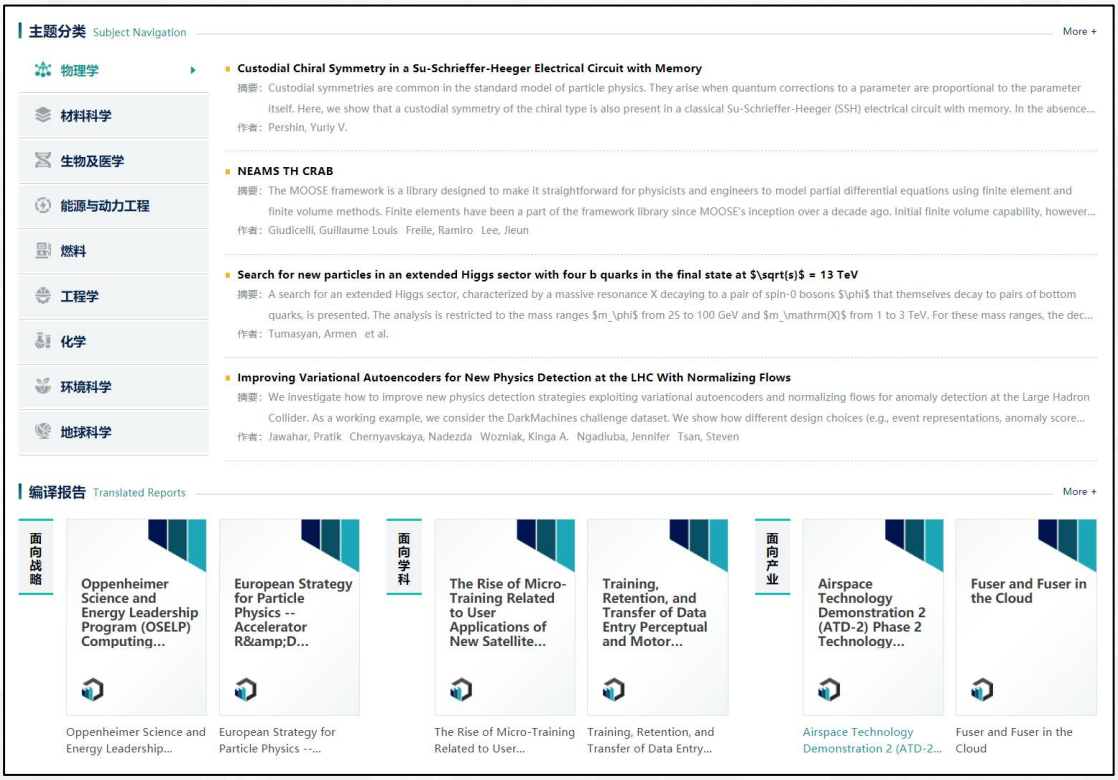

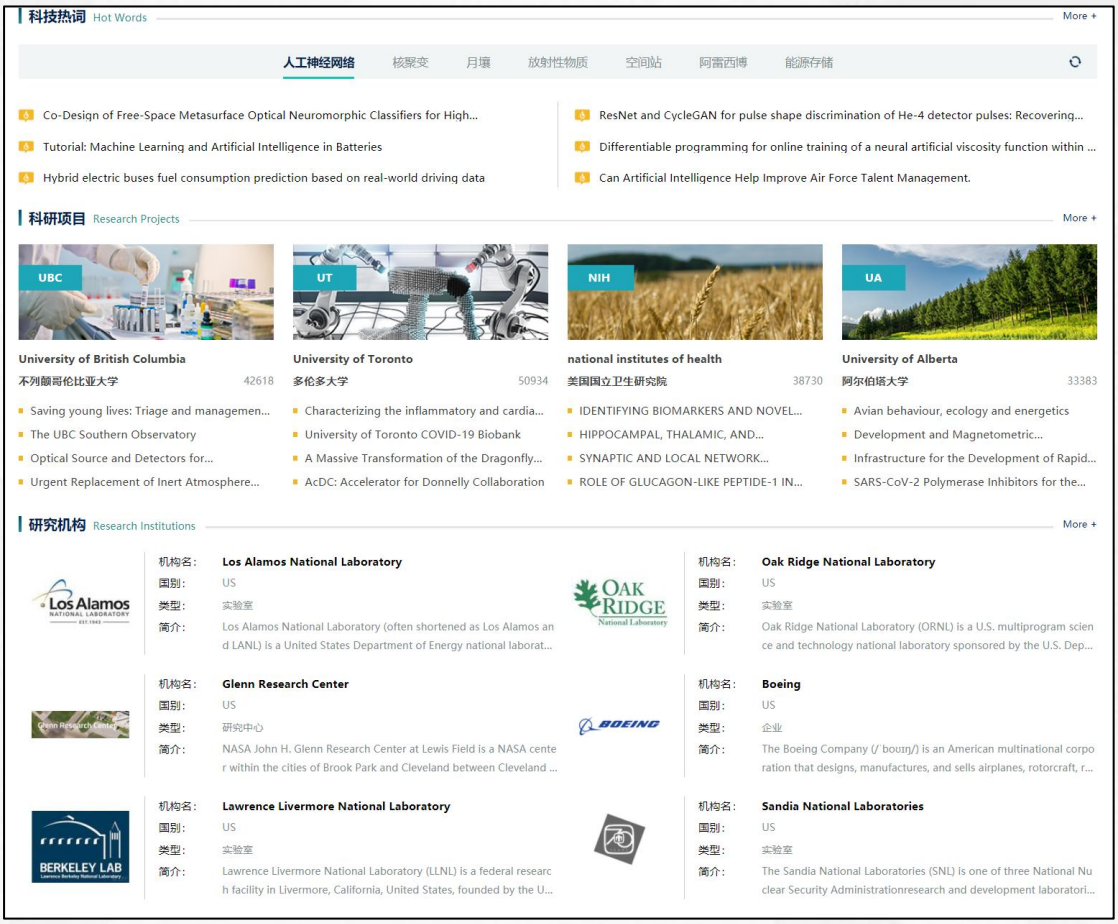

2、快速检索

快速检索提供报告名称、报告号、作者、发布年份、赞助机构、关键词、研究机构和科研项目等检索字段，选择检索字段后输入检索词即可。

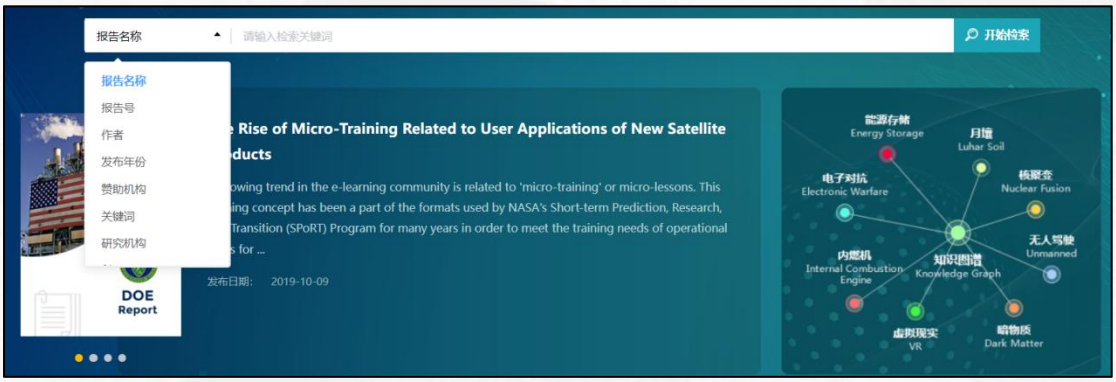

报告检索结果列表页提供年度结果统计表，展示报告出版的年份和数量信息，同时提供来源机构、分类信息、主题词、年份和文档类型的分组聚类，可以进行条件的筛选，使检索结果更加精确。

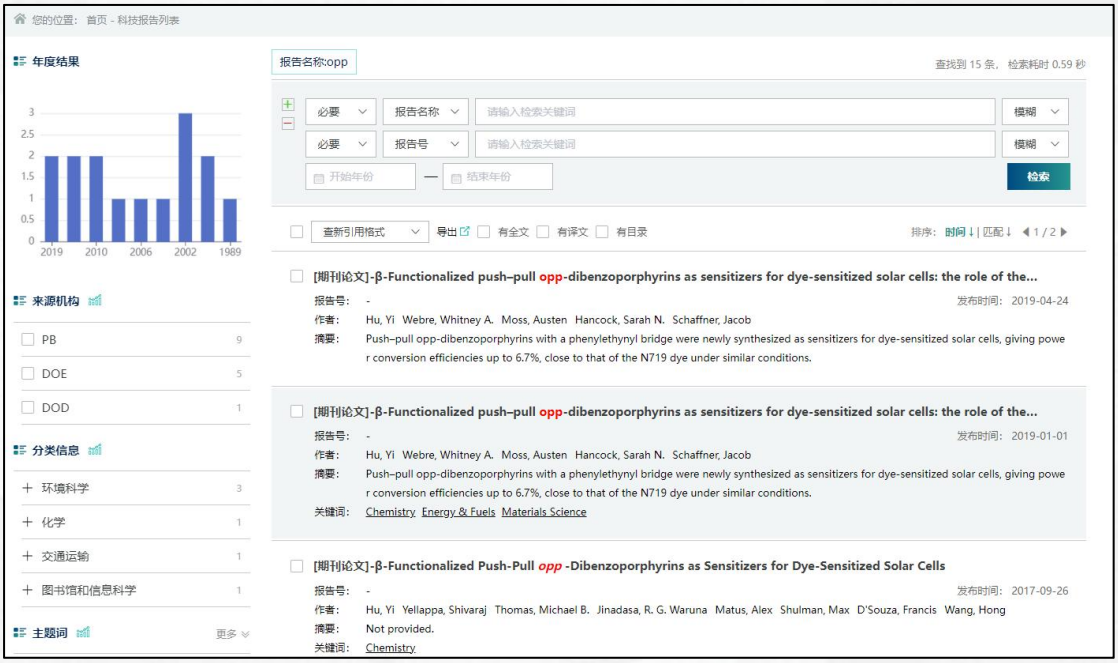

3、知识图谱检索

知识图谱页面默认展示名称含 NASA 的知识图谱节点。提供报告关联图谱信息展示，以报告题目为中心，连接到作者和机构信息；通过信息卡，展示图谱节点相关信息；同时可对图谱进行“全屏/筛选/统计”等操作。

4、主题分类

主题分类列表页可逐级往下进行检索，查看所需类别的科技报告。

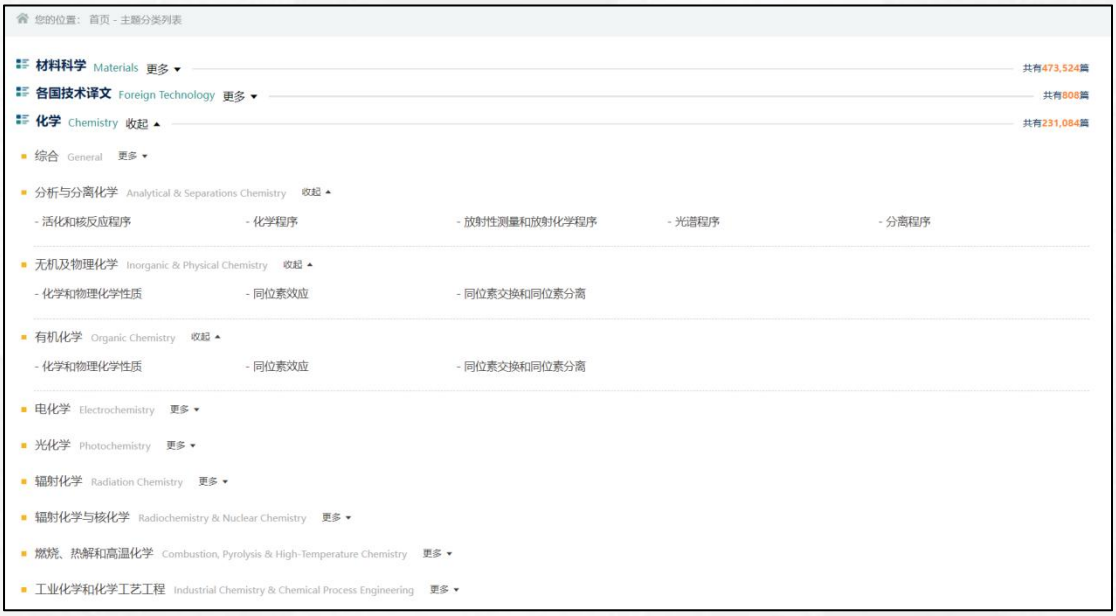

5、研究机构

研究机构列表页提供根据机构字顺进行检索，也可对机构类型进行筛选，精确搜索结果。

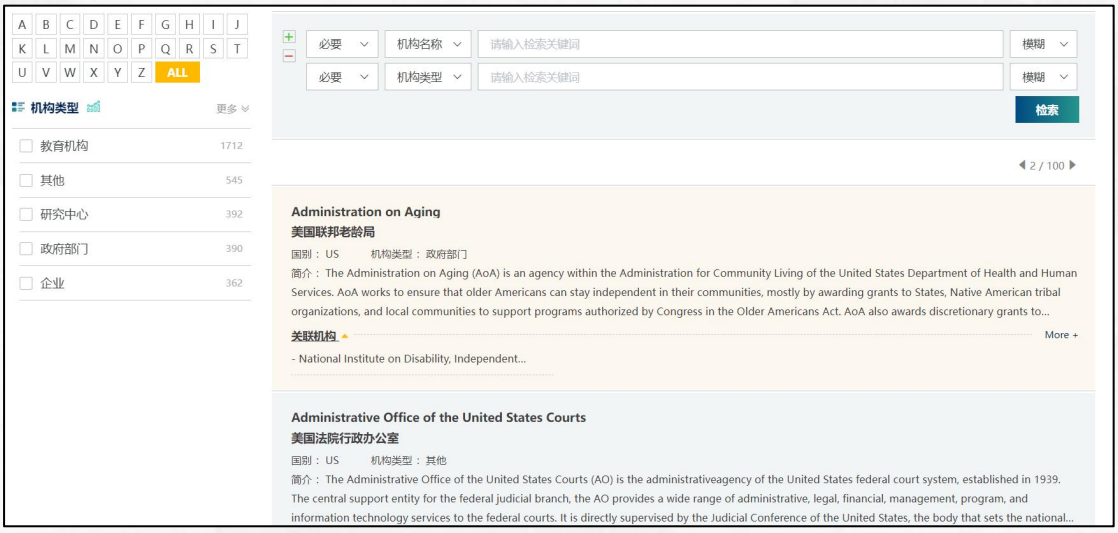

详情页面提供机构的简介、相关信息（包括基本信息、机构关系、人事信息和其他信息）、发文量统计图表、关联机构分类展示，以及机构报告分类展示。

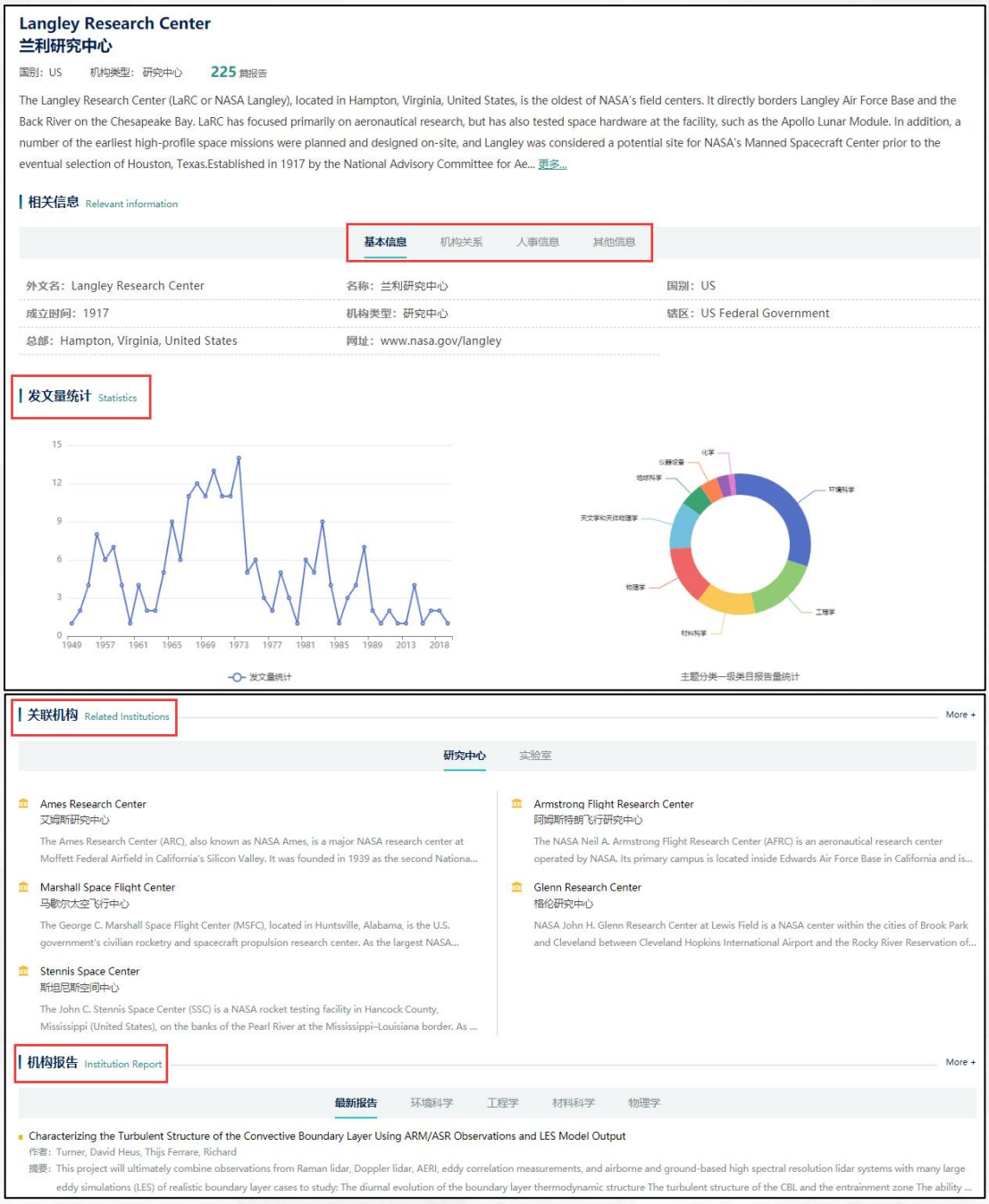

6、科研项目

科研项目列表页提供项目经费、资助来源、开始年份的分组聚类，根据条件进行筛选，精确搜索结果，详情页面提供该科研项目的详细信息。

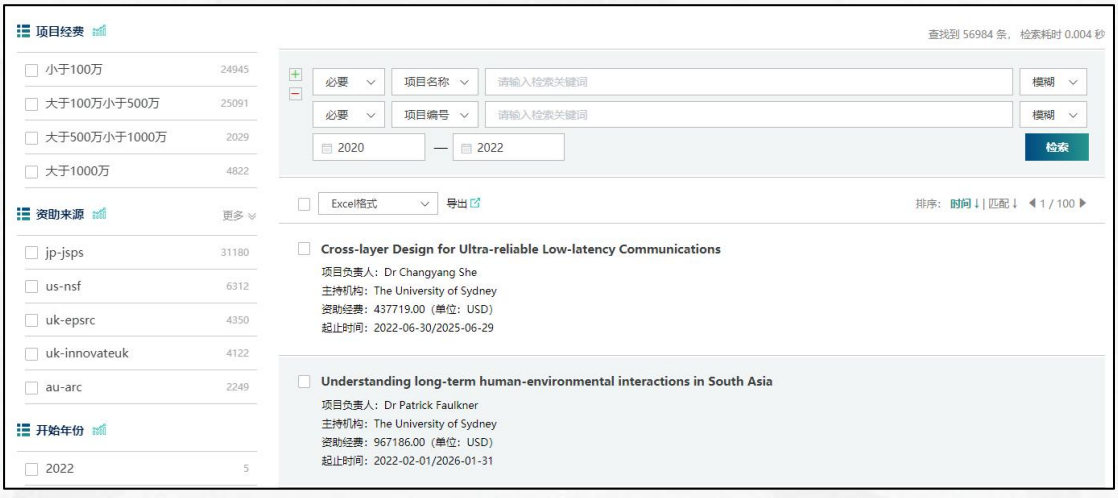

7、高级检索

高级检索页面可实现对检索类型、关键词、年份等的筛选限制，缩小检索范围，使检索结果更加精准。

8、目录预览、报告下载

在报告详情页面，可以对报告的目录进行预览，查看报告的完整目录。

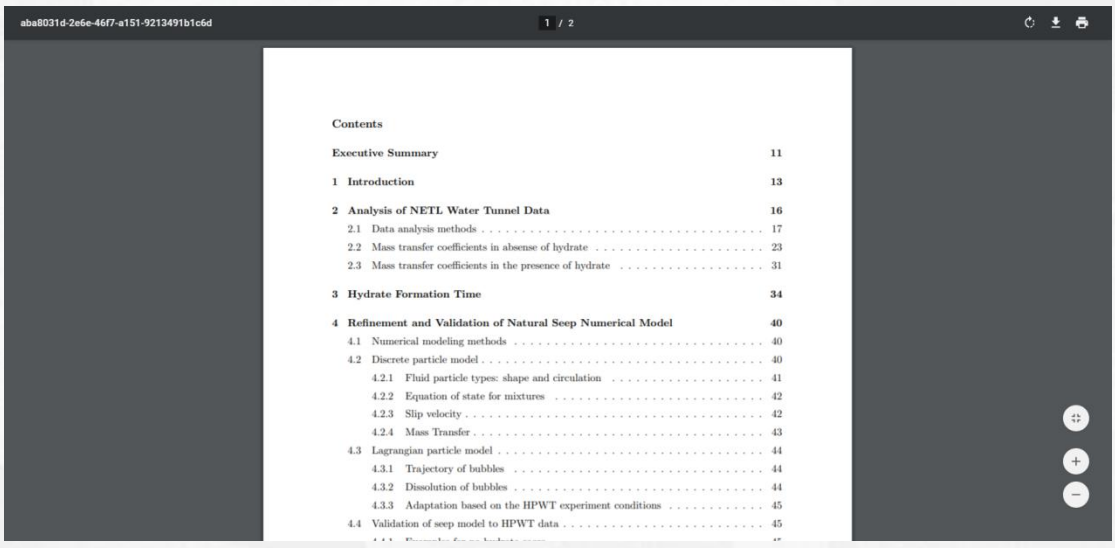

在报告详情页面，对新增的字段进行了展示，如合作机构、报告涵盖时间、合同编号、基金编号、文献类型等多个字段；

提供当前页面参考译文的查看，以及全文预览、全文下载、导出题录等功能；如没有本地全文，还可以进行原文索取。

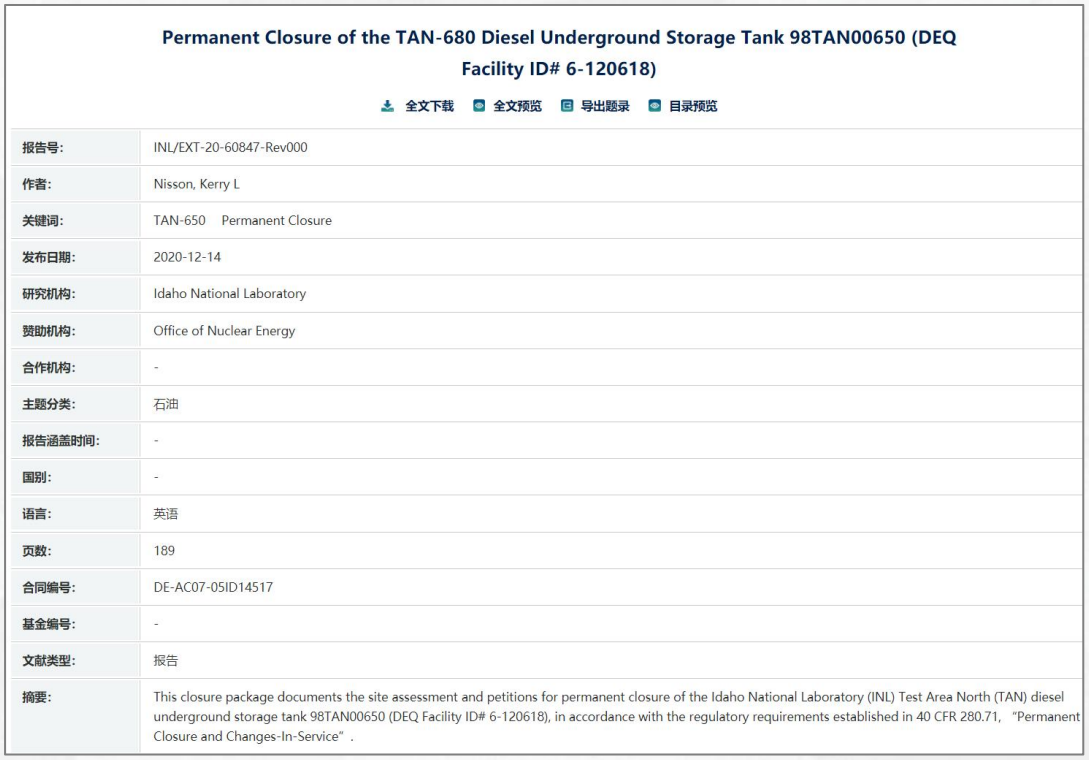

Permanent Closure of the TAN-680 Diesel Underground Storage Tank 98TAN00650 (DEQ Facility ID# 6-120618)

全文下载　全文预览　导出题录　目录预览

报告号:	INL/EXT-20-60847-Rev000
作者:	Nisson, Kerry L
关键词:	TAN-650　Permanent Closure
发布日期:	2020-12-14
研究机构:	Idaho National Laboratory
赞助机构:	Office of Nuclear Energy
合作机构:	-
主题分类:	石油
报告涵盖时间:	-
国别:	-
语言:	英语
页数:	189
合同编号:	DE-AC07-05ID14517
基金编号:	-
文献类型:	报告
摘要:	This closure package documents the site assessment and petitions for permanent closure of the Idaho National Laboratory (INL) Test Area North (TAN) diesel underground storage tank 98TAN00650 (DEQ Facility ID# 6-120618), in accordance with the regulatory requirements established in 40 CFR 280.71, "Permanent Closure and Changes-In-Service".

【七】/ 服务保障

1、订购模式

> 镜像站使用模式	> 网络使用模式	> 数据定制服务
将数据库和检索系统安装在用户本地服务器上，在单位局域网范围内，不限次数使用。	用户通过绑定 IP 地址登录服务系统，获得相关使用权限与服务。	根据用户的不同需求，定制个性化整体方案，提供特色专业服务，辅助用户建立系统进行使用。

2、售后服务

▌服务内容

▌服务方式

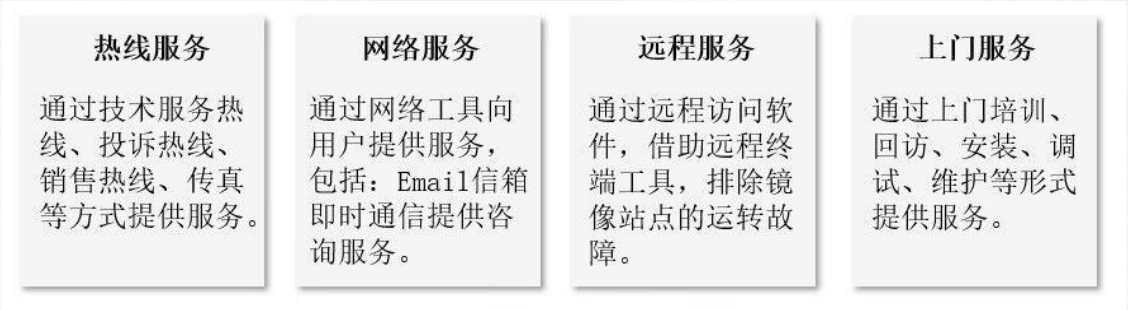

【八】/ 报告样例

“地球物理学”报告样例展示

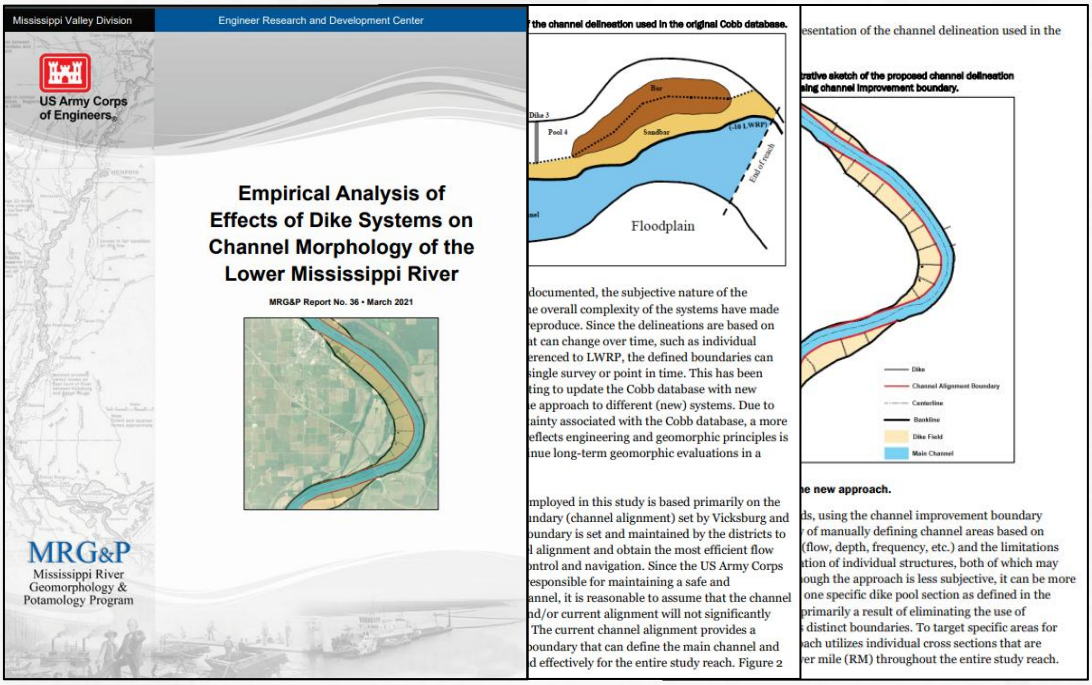

“空气动力学”报告样例展示

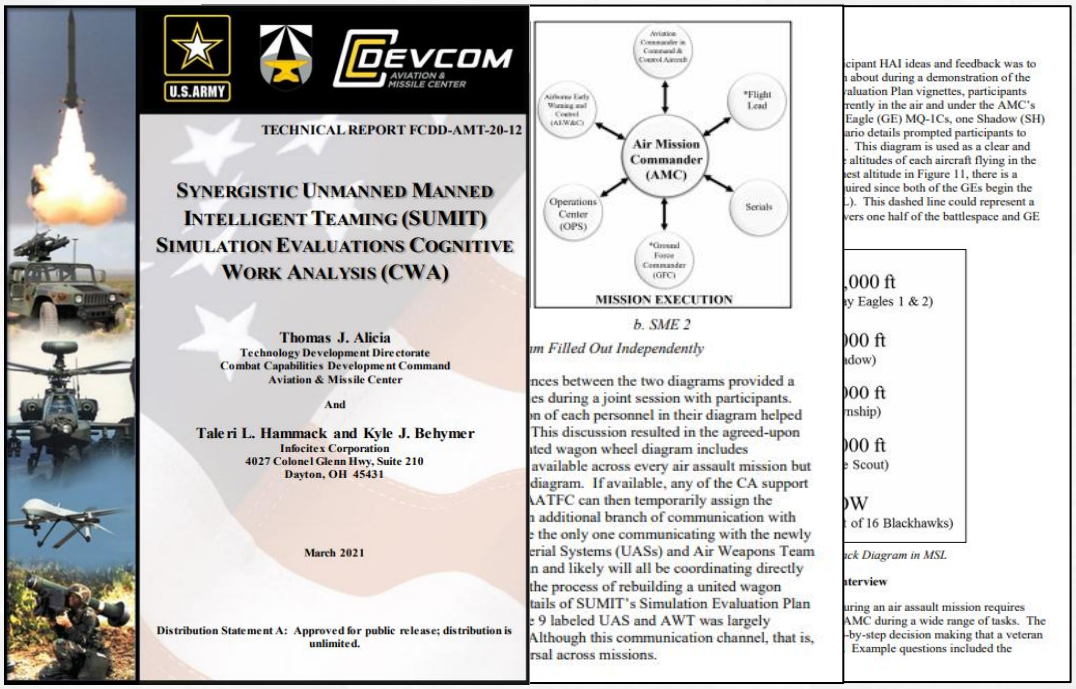

“土木工程”报告样例展示

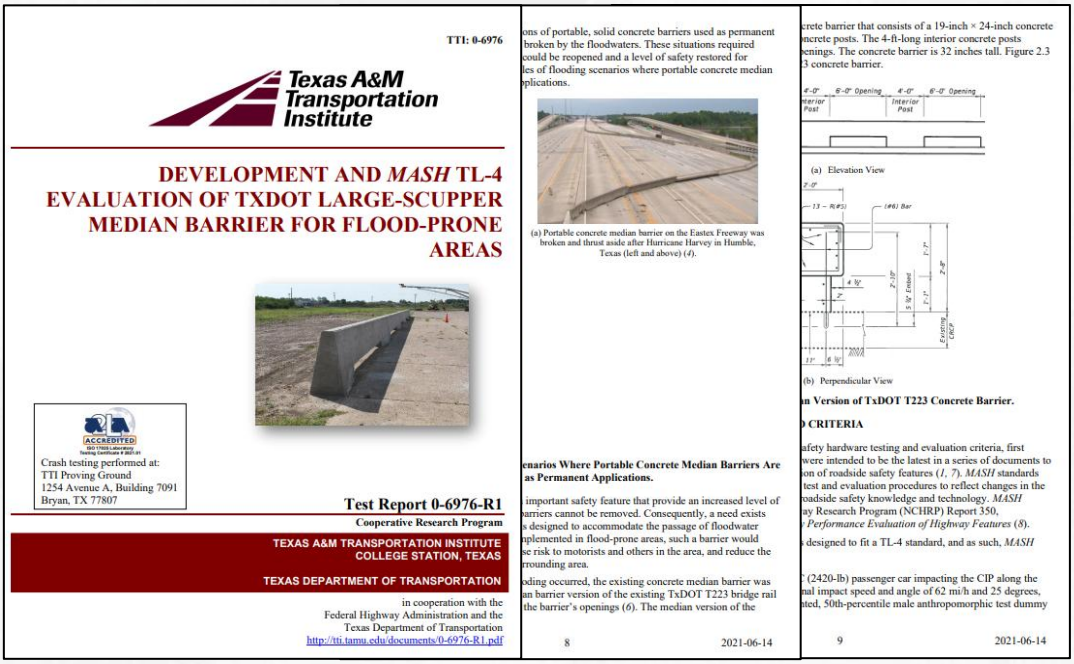

TTI: 0-6976

Texas A&M Transportation Institute

DEVELOPMENT AND *MASH* TL-4 EVALUATION OF TXDOT LARGE-SCUPPER MEDIAN BARRIER FOR FLOOD-PRONE AREAS

Crash testing performed at:
TTI Proving Ground
1254 Avenue A, Building 7091
Bryan, TX 77807

Test Report 0-6976-R1

Cooperative Research Program

TEXAS A&M TRANSPORTATION INSTITUTE
COLLEGE STATION, TEXAS

TEXAS DEPARTMENT OF TRANSPORTATION

in cooperation with the
Federal Highway Administration and the
Texas Department of Transportation
http://tti.tamu.edu/documents/0-6976-R1.pdf

...ons of portable, solid concrete barriers used as permanent ...broken by the floodwaters. These situations required ...could be reopened and a level of safety restored for ...les of flooding scenarios where portable concrete median ...pplications.

(a) Portable concrete median barrier on the Eastex Freeway was broken and thrust aside after Hurricane Harvey in Humble, Texas (left and above) (*4*).

...enarios Where Portable Concrete Median Barriers Are ...as Permanent Applications.

...important safety feature that provide an increased level of ...arriers cannot be removed. Consequently, a need exists ...s designed to accommodate the passage of floodwater ...plemented in flood-prone areas, such a barrier would ...se risk to motorists and others in the area, and reduce the ...rrounding area.

...oding occurred, the existing concrete median barrier was ...an barrier version of the existing TxDOT T223 bridge rail ...the barrier's openings (*6*). The median version of the

8 2021-06-14

...crete barrier that consists of a 19-inch × 24-inch concrete ...ncrete posts. The 4-ft-long interior concrete posts ...enings. The concrete barrier is 32 inches tall. Figure 2.3 ...3 concrete barrier.

(a) Elevation View

(b) Perpendicular View

...n Version of TxDOT T223 Concrete Barrier.

...D CRITERIA

...afety hardware testing and evaluation criteria, first ...were intended to be the latest in a series of documents to ...on of roadside safety features (*1*, *7*). *MASH* standards ...test and evaluation procedures to reflect changes in the ...oadside safety knowledge and technology. *MASH* ...ay Research Program (NCHRP) Report 350, ...*Performance Evaluation of Highway Features* (*8*).

...designed to fit a TL-4 standard, and as such, *MASH*

...(2420-lb) passenger car impacting the CIP along the ...nal impact speed and angle of 62 mi/h and 25 degrees, ...sted, 50th-percentile male anthropomorphic test dummy

9 2021-06-14

“材料科学”报告样例展示

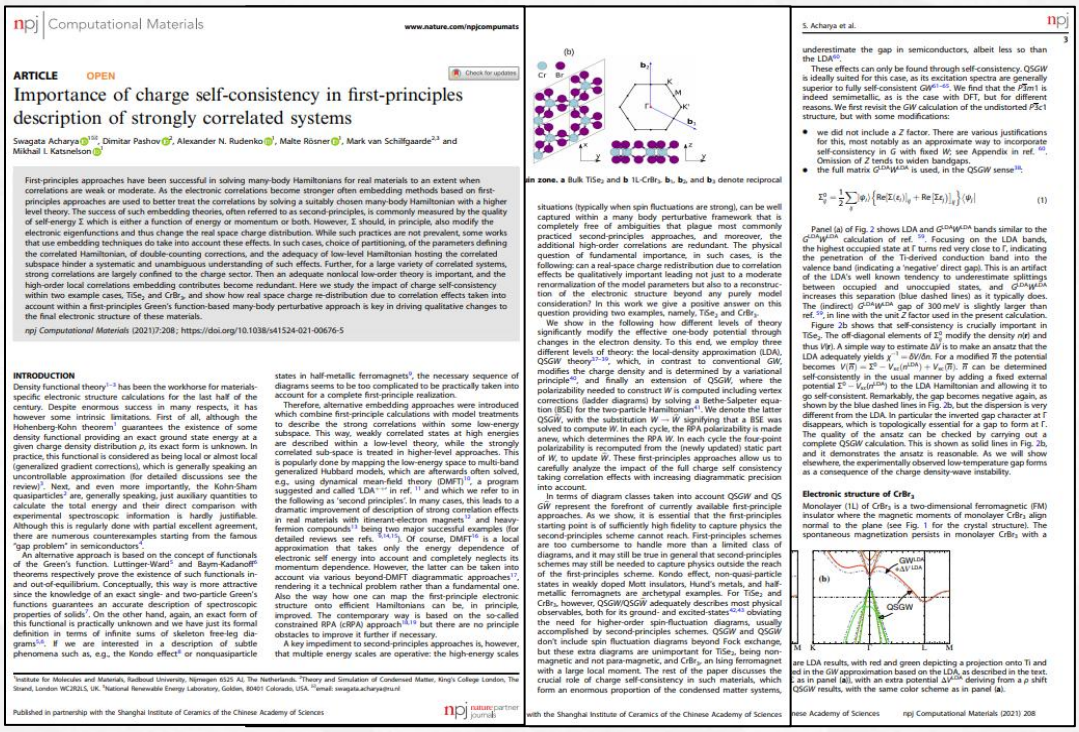

npj | Computational Materials

www.nature.com/npjcompumats

ARTICLE OPEN

Importance of charge self-consistency in first-principles description of strongly correlated systems

Swagata Acharya[1✉], Dimitar Pashov[2], Alexander N. Rudenko[3], Malte Rösner[2], Mark van Schilfgaarde[2,3] and Mikhail I. Katsnelson[3]

First-principles approaches have been successful in solving many-body Hamiltonians for real materials to an extent when correlations are weak or moderate. As the electronic correlations become stronger often embedding methods based on first-principles approaches are used to better treat the correlations by solving a suitably chosen many-body Hamiltonian with a higher level theory. The success of such embedding theories, often referred to as second-principles, is commonly measured by the quality of self-energy Σ which is either a function of energy or momentum or both. However, Σ should, in principle, also modify the electronic eigenfunctions and thus change the real space charge distribution. While such practices are not prevalent, some works that use embedding techniques do take into account these effects. In such cases, choice of partitioning, of the parameters defining the correlated Hamiltonian, of double-counting corrections, and the adequacy of low-level Hamiltonian hosting the correlated subspace hinder a systematic and unambiguous understanding of such effects. Further, for a large variety of correlated systems, strong correlations are largely confined to the charge sector. Then an adequate nonlocal low-order theory is important, and the high-order local correlations embedding contributes become redundant. Here we study the impact of charge self-consistency within two example cases, $TiSe_2$ and $CrBr_3$, and show how real space charge re-distribution due to correlation effects taken into account within a first-principles Green's function-based many-body perturbative approach is key in driving qualitative changes to the final electronic structure of these materials.

npj Computational Materials (2021)7:208 ; https://doi.org/10.1038/s41524-021-00676-5

INTRODUCTION

Density functional theory[1–3] has been the workhorse for materials-specific electronic structure calculations for the last half of the century. Despite enormous success in many respects, it has however some intrinsic limitations. First of all, although the Hohenberg-Kohn theorem[1] guarantees the existence of some density functional providing an exact ground state energy at a given charge density distribution ρ, its exact form is unknown. In practice, this functional is considered as being local or almost local (generalized gradient corrections), which is generally speaking an uncontrollable approximation (for detailed discussions see the review[3]). Next, and even more importantly, the Kohn-Sham quasiparticles[2] are, generally speaking, just auxiliary quantities to calculate the total energy and their direct comparison with experimental spectroscopic information is hardly justifiable. Although this is regularly done with partial excellent agreement, there are numerous counterexamples starting from the famous "gap problem" in semiconductors[3].

An alternative approach is based on the concept of functionals of the Green's function. Luttinger-Ward[4] and Baym-Kadanoff[5] theorems respectively prove the existence of such functionals in- and out-of-equilibrium. Conceptually, this way is more attractive since the knowledge of an exact single- and two-particle Green's functions guarantees an accurate description of spectroscopic properties of solids[3]. On the other hand, again, an exact form of this functional is practically unknown and we have just its formal definition in terms of infinite sums of skeleton free-leg diagrams[5,6]. If we are interested in a description of subtle phenomena such as, e.g., the Kondo effect[6] or nonquasiparticle states in half-metallic ferromagnets[9], the necessary sequence of diagrams seems to be too complicated to be practically taken into account for a complete first-principle realization.

Therefore, alternative embedding approaches were introduced which combine first-principle calculations with model treatments to describe the strong correlations within some low-energy subspace. This way, weakly correlated states at high energies are described within a low-level theory, while the strongly correlated sub-space is treated in higher-level approaches. This is popularly done by mapping the low-energy space to multi-band generalized Hubbard models, which are afterwards often solved, e.g., using dynamical mean-field theory (DMFT)[10], a program suggested and called 'LDA++' in ref. [11] and which we refer to in the following as 'second principles'. In many cases, this leads to a dramatic improvement of description of strong correlation effects in real materials with itinerant-electron magnets[12] and heavy-fermion compounds[13] being two major successful examples (for detailed reviews see refs. [3,14,15]). Of course, DMFT[10] is a local approximation that takes only the energy dependence of electronic self energy into account and completely neglects its momentum dependence. However, the latter can be taken into account via various beyond-DMFT diagrammatic approaches[17], rendering it a technical problem rather than a fundamental one. Also the way how one can map the first-principle electronic structure onto efficient Hamiltonians can be, in principle, improved. The contemporary way is based on the so-called constrained RPA (cRPA) approach[18,19] but there are no principle obstacles to improve it further if necessary.

A key impediment to second-principles approaches is, however, that multiple energy scales are operative: the high-energy scales

[1]Institute for Molecules and Materials, Radboud University, Nijmegen 6525 AJ, The Netherlands. [2]Theory and Simulation of Condensed Matter, King's College London, The Strand, London WC2R2LS, UK. [3]National Renewable Energy Laboratory, Golden, 80401 Colorado, USA. ✉email: swagata.acharya@ru.nl

Published in partnership with the Shanghai Institute of Ceramics of the Chinese Academy of Sciences

...in zone. **a** Bulk $TiSe_2$ and **b** 1L-$CrBr_3$. $\mathbf{b}_1$, $\mathbf{b}_2$, and $\mathbf{b}_3$ denote reciprocal

situations (typically when spin fluctuations are strong), can be well captured within a many body perturbative framework that is completely free of ambiguities that plague most commonly practiced second-principles approaches, and moreover, the additional high-order correlations are redundant. The physical question of fundamental importance, in such cases, is the following: can a real-space charge redistribution due to correlation effects be qualitatively important leading not just to a moderate renormalization of the model parameters but also to a reconstruction of the electronic structure beyond any purely model consideration? In this work we give a positive answer on this question providing two examples, namely, $TiSe_2$ and $CrBr_3$.

We show in the following how different levels of theory significantly modify the effective one-body potential through changes in the electron density. To this end, we employ three different levels of theory: the local-density approximation (LDA), QSGW theory[37–39], which, in contrast to conventional *GW*, modifies the charge density and is determined by a variational principle[40], and finally an extension of QSGW, where the polarizability needed to construct W is computed including vertex corrections (ladder diagrams) by solving a Bethe-Salpeter equation (BSE) for the two-particle Hamiltonian[41]. We denote the latter QSG$\hat{W}$, with the substitution $W \to \hat{W}$ signifying that a BSE was solved to compute W. In each cycle, the RPA polarizability is made anew, which determines the RPA W. In each cycle the four-point polarizability is recomputed from the (newly updated) static part of W, to update $\hat{W}$. These first-principles approaches allow us to carefully analyze the impact of the full charge self consistency taking correlation effects with increasing diagrammatic precision into account.

In terms of diagram classes taken into account QSGW and QS*GW* represent the forefront of currently available first-principle approaches. As we show, it is essential that the first-principles starting point is of sufficiently high fidelity to capture physics the second-principles scheme cannot reach. First-principles schemes are too cumbersome to handle more than a limited class of diagrams, and it may still be true in general that second-principles schemes may still be needed to capture physics outside the reach of the first-principles scheme. Kondo effect, non-quasi-particle states in weakly doped Mott insulators, Hund's metals, and half-metallic ferromagnets are archetypal examples. For $TiSe_2$ and $CrBr_3$, however, QSGW/QSG$\hat{W}$ adequately describes most physical observables, both for its ground- and excited-states[42,43] obviating the need for higher-order spin-fluctuation diagrams, usually accomplished by second-principles schemes. QSGW and QSG$\hat{W}$ don't include spin fluctuation diagrams beyond Fock exchange, but these extra diagrams are unimportant for $TiSe_2$, being non-magnetic and not para-magnetic, and $CrBr_3$, an Ising ferromagnet with a large local moment. The rest of the paper discusses the crucial role of charge self-consistency in such materials, which form an enormous proportion of the condensed matter systems,

underestimate the gap in semiconductors, albeit less so than the LDA[40].

These effects can only be found through self-consistency. QSGW is ideally suited for this case, as its excitation spectra are generally superior to fully self-consistent *GW*[41–45]. We find that the $P\bar{3}m1$ is indeed semimetallic, as is the case with DFT, but for different reasons. We first revisit the *GW* calculation of the undistorted $P\bar{3}c1$ structure, but with some modifications:

- we did not include a Z factor. There are various justifications for this, most notably as an approximate way to incorporate self-consistency in G with fixed W; see Appendix in ref. [60]. Omission of Z tends to widen bandgaps,
- the full matrix $G^{LDA}W^{LDA}$ is used, in the QSGW sense[38],

$$\Sigma^0_{ij} = \frac{1}{2}\sum_q \psi_i \left\{ \mathrm{Re}[\Sigma(\epsilon_i)]_{ij} + \mathrm{Re}[\Sigma_i]_{ij} \right\} \langle \psi_j | \qquad (1)$$

Panel (a) of Fig. 2 shows LDA and $G^{LDA}W^{LDA}$ bands similar to the $G^{LDA}W^{LDA}$ calculation of ref. [59]. Focusing on the LDA bands, the highest occupied state at Γ turns red very close to Γ, indicating the penetration of the Ti-derived conduction band into the valence band (indicating a 'negative' direct gap). This is an artifact of the LDA's well known tendency to underestimate splittings between occupied and unoccupied states, and $G^{LDA}W^{LDA}$ increases this separation (blue dashed lines) as it typically does. The (indirect) $G^{LDA}W^{LDA}$ gap of 300 meV is slightly larger than ref. [59], in line with the unit Z factor used in the present calculation.

Figure 2b shows that self-consistency is crucially important in $TiSe_2$. The off-diagonal elements of Σ^0_{ij} modify the density $n(\mathbf{r})$ and thus $V(\mathbf{r})$. A simple way to estimate ΔV is to make an ansatz that the LDA adequately yields $\chi^{-1} - \delta V/\delta n$. For a modified $\tilde{n}$ the potential becomes $V(\tilde{n}) = \Sigma^0 - V_{xc}(n^{LDA}) + V_{xc}(\tilde{n})$. $\tilde{n}$ can be determined self-consistently in the usual manner by adding a fixed external potential $\Sigma^0 - V_{xc}(n^{LDA})$ to the LDA Hamiltonian and allowing it to go self-consistent. Remarkably, the gap becomes negative again, as shown by the blue dashed lines in Fig. 2b, but the dispersion is very different from the LDA. In particular the inverted gap character at Γ disappears, which is topologically essential for a gap to form at Γ. The quality of the ansatz can be checked by carrying out a complete QSGW calculation. This is shown as solid lines in Fig. 2b, and it demonstrates the ansatz is reasonable. As we will show elsewhere, the experimentally observed low-temperature gap forms as a consequence of the charge density-wave instability.

Electronic structure of $CrBr_3$

Monolayer (1L) of $CrBr_3$ is a two-dimensional ferromagnetic (FM) insulator where the magnetic moments of monolayer $CrBr_3$ align normal to the plane (see Fig. 1 for the crystal structure). The spontaneous magnetization persists in monolayer $CrBr_3$ with a

...are LDA results, with red and green depicting a projection onto Ti and ...ed in the *GW* approximation based on the LDA, as described in the text. ...as in panel (**a**), with an extra potential ΔV^{LDA} deriving from a ρ shift ...QSGW results, with the same color scheme as in panel (**a**).

【九】/ 正式用户

高等院校

清华大学	浙江大学
中国科学技术大学	国防科技大学
西北工业大学	中国民航大学
重庆大学	大连理工大学
合肥工业大学	中山大学
天津大学	中国矿业大学
江苏师范大学	电子科技大学
内蒙古大学	西南科技大学
西南交通大学	东北大学
湖南大学	广东工业大学
福州大学	河南大学
上海海洋大学	……

情报系统/科研机构

山东省科学技术情报研究院	天津市科学技术信息研究所
河北省科学技术情报研究院	钢铁研究总院
丽水市科技信息中心	南宁市科学技术情报研究院
山西省科学技术情报研究所科技查新中心	四川省科技信息研究所
解放军总参谋部第 57 研究所	中国航空工业第一飞机设计研究院
中国航天员科研训练中心	国家海洋局第一海洋研究所
江苏省科学技术情报研究所	贵州省科学技术情报研究所
中国科学院武汉文献情报中心	……

【十】/ 联络我们

地　　址：重庆市两江新区黄山大道水星大厦 B 座 16 层　　传　　真：(023) 67033861

销售热线：(023) 86815037　86815002　　免费电话：400-636-0093

公司网址：http://about.sunwayinfo.com.cn　　邮　　编：401121